# EV6: Experimental Validation of Sensor Interaction Compensation Scheme for Microwave Imaging

Olivier Franza[1] *, Nadine Joachimowicz and Jean-Charles Bolomey

Electromagnetic Department, Supélec-CNRS, 91192 Gif-sur-Yvette, FRANCE
[1] currently at Intel Corporation, 334 South St., Shrewsbury, MA 01545, USA
e-mail: Olivier.Franza@intel.com, Bolomey@supelec.fr

## I. Introduction

Microwave tomography theory has been radically improved by the development of iterative non-linear reconstruction algorithms (NLRA). However, unless tailored to a specific problem, they rarely provide satisfactory answers when the presence of sensors is non-negligible experimentally. At most, it is assumed that a linear relation holds between the measurement data given by the sensors and the field in which they are placed. The sensor interaction compensation scheme (SICS) was developed [1] with the unambiguous scope of formally modeling measurement systems within the reconstruction algorithm to fully compensate perturbations resulting from sensor presence, and applied to a Newton-Kantorovich technique (NKT). In this paper, after a brief review of the method, the experimental validation of SICS (EV6) is presented for both direct and inverse scattering problems using data from two measurement setups: an open-space modulated scattering system [2] and a water-filled microwave scanner [3].

## II. NKT-based SICS

The NKT was developed at the end of the 1970s [4] and was applied to microwave imaging [5] at the beginning of the 1990s. Its derivation starts with the electric field integral equation (EFIE) which non-linearly relates the total electric field $\mathbf{E}$ to the contrast $\overline{\mathbf{C}}$ of an object with respect to the background through an integral equation, containing the free-space Green's function kernel $\overline{\mathbf{K}}$. By using the method of moments, a generic matrix equation is derived:

$$\mathbf{E} = \mathbf{E}^i + \overline{\mathbf{K}}\ \overline{\mathbf{C}}\ \mathbf{E} \tag{1}$$

where $\mathbf{E}^i$ is the incident electric field without object. Depending on the observation position, both the coupling equation inside the object domain O and the observation equation at measurement locations $\Omega$, where the sensors are located, are derived from Equation (1). The observation equation is expressed in terms of the scattered field, $\mathbf{E}^s_\Omega = \mathbf{E}_\Omega - \mathbf{E}^i_\Omega$, the field difference with and without the object. Classically, $\mathbf{E}^i_\Omega$ is the incident wave illuminating the object. As shown by the non-shaded regions in Figure 1, the NKT iterative process is then implemented as such:

- contrast initialization with or without *a priori* information;
- computation of the field inside the object for a given contrast (forward problem);
- computation of the scattered field at the measurement points $\mathbf{E}^s_\Omega$;
- comparison between the computed and measured scattered fields $\delta\mathbf{E}^s_\Omega$;
- computation to the first order of the correction on the contrast $\delta\overline{\mathbf{C}}_\mathrm{O}$;
- update of the contrast and return to the second step until a stability criterion is reached for the error on the scattered field.

0-7803-7846-6/03/$17.00 

The computation of the correction on the contrast $\delta\mathbf{C}_\mathrm{O}$ is ill-conditioned and is where the main complexity of the method lies [1], [5]. It is not the subject of this paper and therefore will not be developed. To formally include sensor coupling and interaction effects, the coupling equation has to encompass both object and sensor domains $\mathrm{O}' = \mathrm{O} \cup \Omega$. From Equation (1), when an object is present, the observation equation becomes:

$$\mathbf{E}_\Omega = \mathbf{E}^i_\Omega + \overline{\mathbf{K}}_{\Omega,\mathrm{O}}\ \overline{\mathbf{C}}_\mathrm{O}\ \mathbf{E}_\mathrm{O} + \overline{\mathbf{K}}_{\Omega,\Omega}\ \overline{\mathbf{C}}_\Omega\ \mathbf{E}_\Omega \tag{2}$$

and when there is no object:

$$\mathbf{E}^\#_\Omega = \mathbf{E}^i_\Omega + \overline{\mathbf{K}}_{\Omega,\Omega}\ \overline{\mathbf{C}}_\Omega\ \mathbf{E}^\#_\Omega \tag{3}$$

where $\mathbf{E}^\#$ is the total field without object. In order to use classical NLRA, an *equivalent* scattered field $\mathbf{E}^d_{\Omega\ eq} = \overline{\mathbf{K}}_{\Omega,\mathrm{O}}\ \overline{\mathbf{C}}_\mathrm{O}\ \mathbf{E}_\mathrm{O}$ is defined to formally match the classical expression of the scattered field. Combining Equations (2) and (3) yields:

$$\mathbf{E}^d_{\Omega\ eq} = \Delta\mathbf{E}_\Omega - \overline{\mathbf{K}}_{\Omega,\Omega}\ \overline{\mathbf{C}}_\Omega\ \Delta\mathbf{E}_\Omega \tag{4}$$

where $\Delta\mathbf{E}_\Omega = \mathbf{E}_\Omega - \mathbf{E}^\#_\Omega$ is the variation of the total field inside the sensors resulting from the introduction of the object. The shaded areas in Figure 1 show the additional steps for SICS. EV6 is presented in the next two sections.

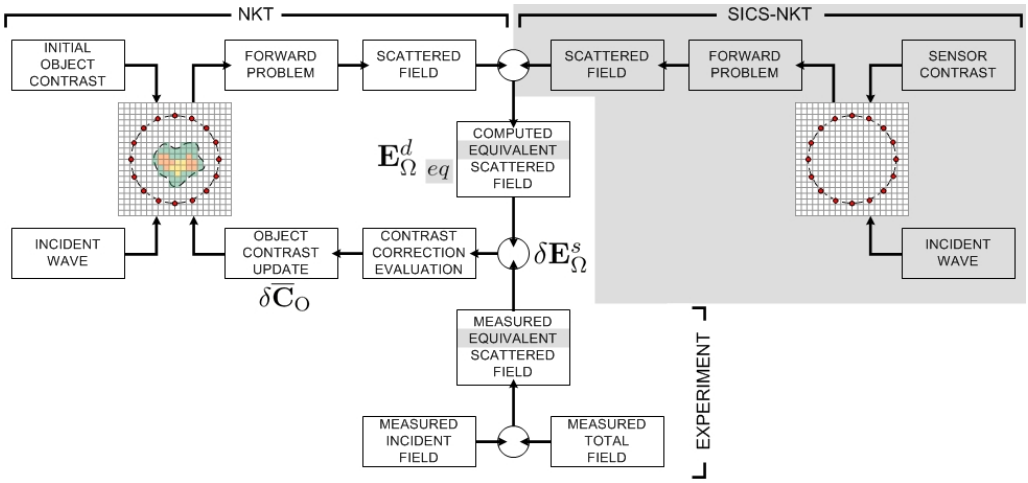


Fig. 1. Reconstruction algorithm diagram.

## III. Open-space 3GHz modulated scattering system

The system[1] in Figure 2 was developed at the Department of Biophysical and Electronical Engineering of the University of Genoa (Italy) [2] and uses the modulated scattering technique [6]. An array of 27 printed-circuit $\frac{\lambda}{4}$ dipoles separated by a distance of $\frac{\lambda}{3}$ on a rectangular dielectric sheet is mechanically displaced around the test area in front of a receiving antenna with a very large aperture (ensuring a quasi uniform measurement). The transmitting antenna, a $\frac{\lambda}{4}$ dipole associated with a plane reflector, generates an almost TM polarized incident wave.

In [2], the modeling of the problem mixes the classical EFIE from Equation (1) and analytical expressions of the field scattered by a small electric dipole [7]. This method accounts for the interactions of the object on the active sensor, but neither the interactions of the object on the passive sensors, nor the ones of the sensors on

[1]The photograph was kindly provided by S. Caorsi, G. L. Gragnani and M. Pastorino.

the object or between themselves. In EV6, dipoles are modeled by circular cylinders of conductivity $\sigma = 10^6$S/m and radius $r = \frac{\lambda}{30}$.

Figure 3 shows a plot of the total field at the sensors; experimental data and E6 simulations for different noise levels are in good agreement. Experimental reconstructions were not performed as this system was phased out by a new one.

## IV. Water-filled 434MHz microwave scanner

The system in Figure 4 was developed at the Electromagnetic Department of Supélec (France) [3]. It is a biomedical microwave imaging system composed of a 59cm-diameter metallic cylinder immersed in water and constituted of 64 multiplexed H-type E-polarized antennas.

Previously, the cylinder was numerically modeled by computing the Green's function of a perfectly circular metallic cavity [3], for all possible distances within. EV6, on the other hand, is more versatile and convenient: the cylinder is modeled with 200 contiguous sensors ($\sigma = 10^6$S/m, $r = \frac{\lambda}{30}$) as shown in Figure 4. Three incident angles 120 degrees apart and 64 measurement points are used. The simulated and measured total fields are compared on Figure 5 and are in good agreement.

The test object is an homogeneous cylinder of dielectric characteristic (54.20,38.40). The square discretization region contains $20 \times 20$ $\frac{\lambda}{10}$ cells. Figure 6 shows the results obtained with *a priori* knowledge of the object's permittivity range (between 0 and 100). From iteration 4, the algorithm converges towards the solution. These results are similar to those of [3], where, using a custom-made triangular inhomogeneous mesh, only the object was discretized.

## V. Conclusion

SICS, through the concept of equivalent scattered field, formally integrates sensor coupling and interaction effects. In this paper, both forward and inverse scattering problems were validated with experimental data. It is now possible to experimentally reconstruct complex permittivity profiles using classical NLRA when the presence of sensors is non-negligible, allowing significant reductions in model noise. EV6 versatility is furthermore established by its extensive modeling capability: both open-space modulated scattering system and water-filled microwave scanner were successfully simulated. Directions for future work include modeling other existing experimental systems and developing higher dimension algorithms.

## References


[1] O. Franza, N. Joachimowicz and J. Ch. Bolowey, "SICS: A Sensor Interaction Compensation Scheme for Microwave Imaging," *IEEE Trans. AP*, vol. 50, pp. 211-216, Feb. 2002.

[2] S. Caorsi, G. L. Gragnani and M. Pastorino, "A multiview microwave imaging system for two-dimensional penetrable objects," *IEEE Trans. MTT*, vol. 39, pp. 845-851, May 1991.

[3] J. M. Geffrin, "Imagerie microondes: étude d'un scanner à 434MHz pour applications biomédicales," Thèse de doctorat, Université d'Orsay-Paris XI, 1995.

[4] R. Roger, D. Maystre and M. Cadilhac, "On a problem of inverse scattering in optics: the dielectric inhomogeneous medium," *Journal Optics*, vol. 2, pp. 83-90, Feb. 1978.

[5] N. Joachimowicz, Ch. Pichot and J. P. Hugonin, "Inverse scattering: an inverse numerical method for electromagnetic imaging," *IEEE Trans. AP*, vol. 39, pp. 1742-1754, Dec. 1991.

[6] J. H. Richmond, "A modulated scattering technique for measurement of field distributions," *IRE Trans. MTT*, vol. MTT-3, pp. 13-15, Jul. 1955.

[7] R. Collin and F. Zucker, "Antenna Theory - Part 1," New York, NY: Mac Graw Hill, 1969.

Fig. 2. Open-space 3GHz system.

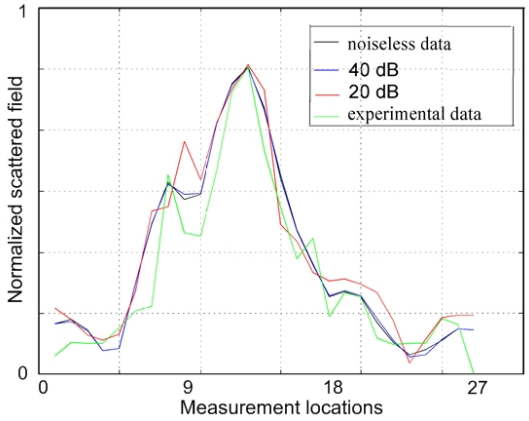


Fig. 3. Scattered fields on the sensors array.

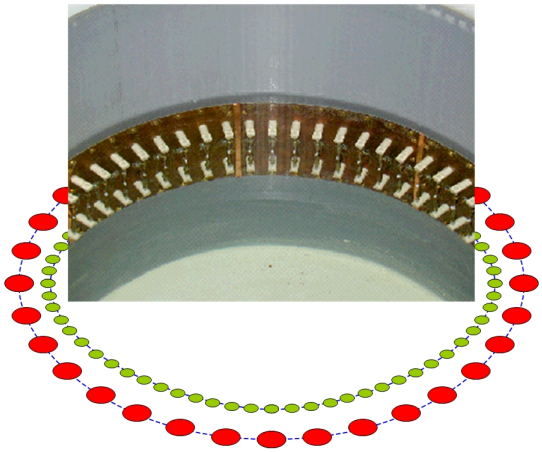

Fig. 4. 434MHz scanner and EV6 modeling.

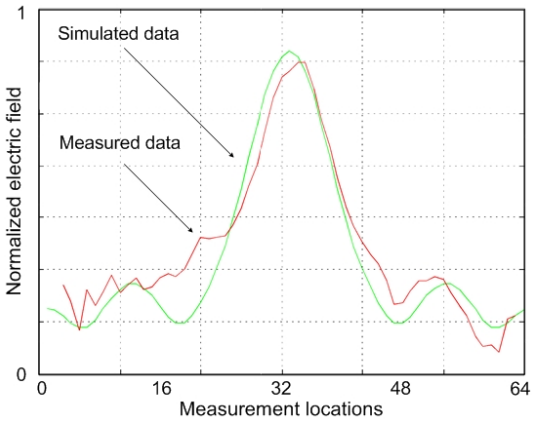


Fig. 5. Total field comparisons.

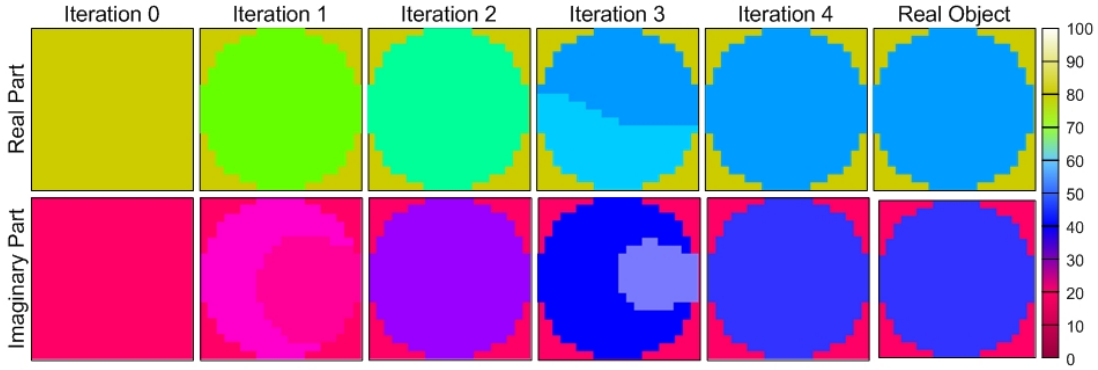


Fig. 6. Experimental reconstruction results.